

**Study of Resistive Plate Chambers  
Scintillation Detectors  
And  
Reconstruction of muon tracks in RPCs**

**Submitted as a Visiting Student to TIFR**

**By  
Medha Soni  
MSc Physics Student  
IIT Madras**

**Under the guidance of  
Professor Sudeshna Banerjee**

# Contents

- ❖ Introduction
- ❖ Resistive Plate Chambers
- ❖ Pictures of TIFR labs where data was taken
- ❖ Scintillation Detectors
- ❖ Photomultiplier Tubes
- ❖ Discriminators
- ❖ Analog to Digital Convertors
- ❖ Charge Histograms
- ❖ Characteristics of RPCs:
  - V-I Characteristics
  - Efficiency and Noise Rate
- ❖ Hit Data plots
- ❖ Tracking Algorithm
- ❖ Histograms for the hit layers
- ❖ Chisquare Plot
- ❖ Residual Plots
- ❖ Tracks along with the hit data
- ❖ Results and Discussions

# Introduction

The India-based neutrino observatory (INO) is a multi-institutional collaboration to set up an Iron Calorimeter to detect atmospheric neutrinos and study their properties.

The INO uses resistive plate chambers as track detectors. Resistive plate chambers are gas based detectors that detect particles passing through it. The particles ionise the gas and hence they are detected. The detector is made of a material with high bulk resistivity and is kept at a high voltage.

Scintillation detectors are also used to detect charged particles. The particles excite the atoms/molecules that make up the scintillator causing a flash of light to be emitted. This light signal is then converted to photo-electrons which is then amplified to give strong electrical signals which are analyzed.

This report presents the work I did as an intern under the Visiting Summer Research Programme (VSRP) 2012 which involved characterisation of the resistive plate chambers, i.e. study of its V-I characteristics, efficiency and noise rate, study of the charge distributed by muons in the scintillators and reconstruction of muon tracks in the RPCs. I worked in the labs set up for the INO.

## RESISTIVE PLATE CHAMBERS

They are gas based detectors with good spatial and timing resolution.

RPCs are constructed by placing two glass plates parallel to each other and separated by a small gap (about 2 mm). Glass is used because the bulk resistivity of glass is very high about  $10^{10}$  to  $10^{12}$   $\Omega\text{-cm}$ . The discharge produced after avalanche is limited to a tiny area of about  $0.1\text{cm}^2$  due to the high resistivity of the glass electrodes. The separation is ensured by poly-carbonate button spacers placed in a grid like pattern. The four sides of the gap are then sealed. A suitable gas mixture, (Freon, isobutane,  $\text{SF}_6$  in this case), one which produces electron-ion pairs and thus a signal when an ionizing particle passes through, is flown through the gap by a gas mixing unit. The outer surfaces of the glass plates are coated with a conductive coating (of graphite). Graphite is used because it has high conductivity, chemical resistance and good mechanical properties. Graphite forms no compounds due to corrosion, no protective surface films as do many metals. A high electric field of about 10kV is applied across these electrodes. Positive voltage is applied to one side and a roughly equal and negative voltage to the other side (for safety purposes). Two Mylar sheets of the same size and thickness 100  $\mu\text{m}$  are placed just above this to provide better isolation. Pick up panels are placed over the Mylar sheet one set along X-direction another over Y-direction. The width of the pickup strip is 3 cm each.

### Gas Mixture used in the glass gap

**Freon:** It absorbs the charged particles before any further avalanche is produced. R134a is used, since it is environment friendly.

**Isobutane:** Since it is an organic gas, it is used to absorb photons from recombination process, limiting the formation of secondary avalanche from primary ionization. It is because of this property is known as Quenching Gas.

**$\text{SF}_6$ :**  $\text{SF}_6$  is used to trap the excess energetic electrons from the gas volume before they can initiate a new avalanche.

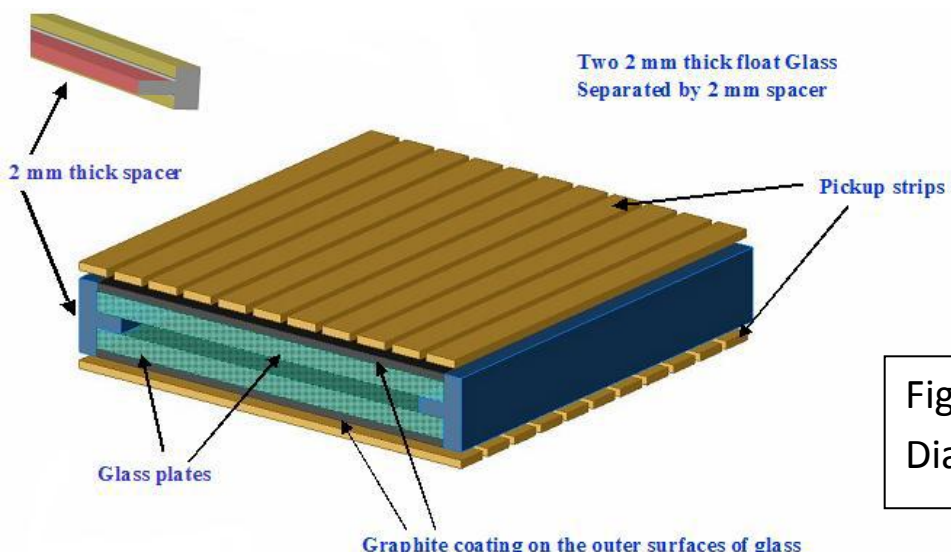


Fig 1: Schematic Diagram of an RPC

## Modes of Operation

There are two modes of operation for RPCs

- **Avalanche Mode:**

Ionized particles, created by primary ionization of gas through charged particles, are accelerated by the electric field and in their way to the electrodes they ionize the gas again to set in an Avalanche process. However this process stops as the internal opposite field is balanced by the external field and the charges are collected in the respective electrodes. The pulse height in this mode is of the order of few milli volts and amplifiers are required in this mode of operation. This mode is also called proportional mode.

- **Streamer Mode:**

In this mode of operation, the electric field inside the gap is kept intense enough to generate limited discharges localized near the crossing point of the ionizing particle. Since this mode is operated at very high voltages, the secondary ionization continues until there is a breakdown of the gas and a continuous discharge takes place. The avalanche is followed by a streamer discharge and signal generated is large of the order few hundreds of milli volts. Hence no amplifiers are needed. Thus, the readout of Streamer mode RPCs is quite simple. However, this mode decreases the life of the detector severely; hence the avalanche mode is preferred. The gas mixture has Freon: Argon: Isobutane in the ratio of 62:30:8 by volume in the streamer mode.

The gas mixture used in the experiment had a composition of

- I. Freon: 95.2%
- II. Iso-butane: 4.5%
- III. SFCs: 0.3%

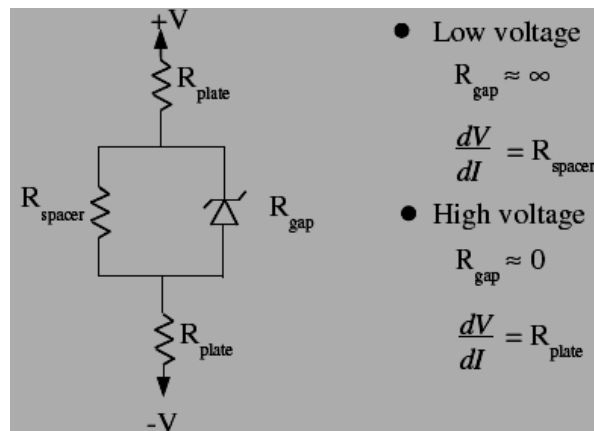


Fig 2:

Circuit diagram for the glass RPCs:

In the low voltage region, it is the spacer resistance that comes into play while in the high voltage region, the glass resistance dominates.



Fig 3: The prototype at TIFR (INO RPC Lab)

It consists of 12 layers of RPCs ( $1m \times 1m$  each) with 32 pickup strips per plane.

This is where the data for the RPC and the scintillator hits was taken.



Fig 4: The  $2m \times 2m$  prototype at TIFR (INO RPC Lab)

It consists of five RPC layers ( $2m \times 2m$ ) each and 64 pickup strips per plane.

The data for the study of V-I characteristics, efficiency and noise rate of the RPCs was collected here.

## SCINTILLATION DETECTORS

The scintillation detectors are probably the most widely used particle detectors in nuclear and particle physics. It makes use of the fact that certain materials when struck by a particle or radiation emit a flash of light i.e scintillation. They are coupled to photomultiplier tubes to give electrical signals which can then be analyzed.

### General Characteristics

A scintillation detector consists of the following components:

- Scintillator
- Photomultiplier
- Light guide (may or may not be present)

### Working

As the particle/radiation passes through the scintillator, it excites the atoms and molecules that make up the scintillator causing light to be emitted. This light is transmitted to the PMT either directly or through a light guide where it is converted into a weak current of photoelectrons which is then further amplified by an electron-multiplier system. In addition, wavelength shifting fibres maybe used. These fibres absorb light from a range of wavelengths and emit light of a particular wavelength, which is more compatible with the PMT.

### Features

- Sensitivity to energy:  
The light output of a scintillator is directly proportional to the exciting energy. Since the photomultiplier is also a linear device, the amplitude of the final electrical signal will also be proportional to this energy.
- Fast time response:  
The response and recovery times of scintillation detectors are short relative to other detectors.
- Pulse Shape Discrimination:  
With certain scintillators, it is possible to distinguish between different types of particles based on the shape of the emitted light pulses. This is due to the excitation of different fluorescence mechanisms by particles of different ionizing power.

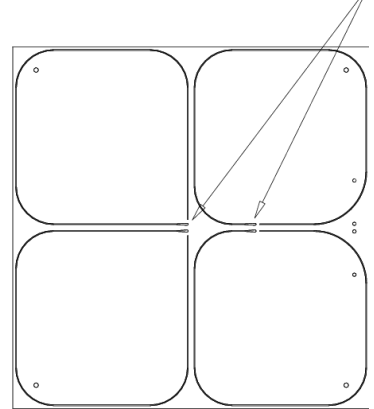
### Properties of a good detector

- High efficiency for converting exciting energy into fluorescent radiation
- Transparency to its fluorescent radiation so as to allow transmission of light
- Emission in a spectral range consistent with the spectral response of the photomultipliers used
- Short decay time

## Types of Scintillators

There are several kinds of scintillators- Inorganic crystals, Organic crystals, Organic liquids, Gaseous, Glass and Plastics. We have used plastic scintillators (Polyvinyl Toluene). The scintillator used had a geometry as shown in Fig

The advantage of using plastic scintillators is that they are cheap, flexible and can be produced in various shapes and sizes. Various types of plastics are used offering differences in light transmission, speed etc.



## Light output response

Fig 5: Scintillator used with four fibres grooved in a sigma shape.

It refers to the efficiency of converting ionization energy to photons. It determines the efficiency and resolution of the scintillator. The response of a scintillator is a function of the type of particle, its energy and also its specific ionization. It is also a function of temperature. This dependence is weak at room temperatures, but should be considered if temperatures very far from normal are to be considered.

The efficiency of the photomultiplier must also be taken into account when considering the efficiency of the scintillation detector since they are coupled. The PMT typically has an efficiency of 30%.

## PHOTOMULTIPLIER TUBES

They are electron tube devices that convert light into a measurable electric current. They are coupled to the scintillator to convert the light into an electric signal.

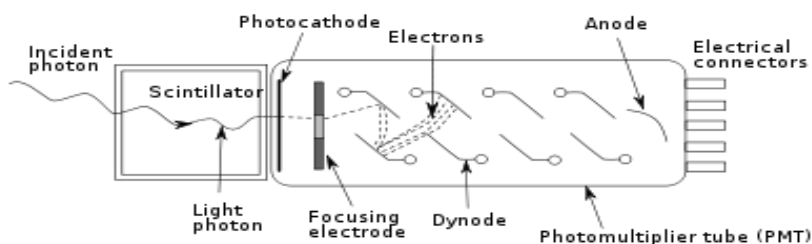


Fig 6: Diagram of the photomultiplier tube

## Construction

It consists of:

- Cathode: It is made of photosensitive material
- Electron multiplier section (or dynode string)
- Anode: This is where the signal can be taken from

## Operation

A high voltage is applied to the cathode, dynodes, and anode such that a potential ladder is set up along the length of the cathode-dynode-anode structure. When an incident photon impinges upon the photocathode, an electron is emitted via the photoelectric effect. Because of the applied voltage, the electron is directed and accelerated towards the first dynode, where upon striking; it transfers some of its energy to the electrons in the dynode. This causes secondary electrons to be emitted, which in turn are accelerated towards the next dynode where more electrons are released and further accelerated. An electron cascade is thus created. At the anode, this cascade is collected to give a current which can then be amplified and analyzed.

When used with a scintillator, it is used in the pulsed mode. In other systems, it can also be used in the continuous mode-under a continuous lumination.

If the cathode and the dynode systems are considered to be linear, the current at the output of the PMT will be directly proportional to the number of incident photons. Hence it is capable of providing information about the particle's presence and also the energy deposited by it in the scintillator.

## NIM STANDARDS

Two types of standards exist: slow-positive and fast-negative logic. The first refers to slow risetime, on the order of hundreds of nanoseconds or more. Fast-negative logic, also referred to as NIM (Nuclear Instruments Module), employs fast signals with risetimes of the order of 1ns and comparable widths.

The first standard established for nuclear and high energy Physics is a modular system called NIM (Nuclear Instruments Module). In this system, the basic electronic apparatus, for example, amplifiers, discriminators etc are constructed in the form of modules according to standard mechanical and electrical specifications. These modules, in turn, fit into NIM bins which supply them with the standard power voltages. The co-axial cables used have a resistance of  $50\Omega$ . The voltage levels for logic 0 and logic 1 are 0V and 800mV respectively. 1m length of the cable causes a delay of 5ns.

## DISCRIMINATORS

The discriminator is a device which responds only to input signals which have a pulse height above a certain threshold value (generally set such that the noise is eliminated). It acts basically as an analog-to-digital-converter. In an ADC, electronic signal is first used to charge a capacitor. The capacitor is then “run down”, i.e. discharged at a constant rate. At the start of the discharge, a scaler counting the pulses from a constant frequency clock or oscillator is gated on. When the capacitor has

completely discharged, the scaler is gated off. The content of the scaler is then a number proportional to the charge on the capacitor.

There are two kinds of discriminators used

- ❖ **Leading Edge Discriminator:** The logic signal is generated at the moment the analog pulse crosses the threshold. This method is inherently subject to the problem of “walk” but can be used with good results if the amplitudes are restricted to a small range.
- ❖ **Constant Fraction Discriminators:** The logic signal is generated at a constant fraction of the peak height to produce an essentially walk-free timing signal. Depending on the type of signal, this level occurs at a constant fraction of the pulse independent of its amplitude.

### Walk and Jitters

The most important factor in any timing system is its resolution. One method to measure the resolution is to measure the time difference of two exactly coincident signals.

The *walk* effect is caused by variations in the amplitude and/or risetime of the incoming signals. Imagine two signals of differing pulse height but exactly coincident in time. Due to the difference in pulse height, the two signals will trigger the discriminator at different times even though they are exactly coincident. This dependence on amplitude causes the signal to *walk* about. A second source of *walk*, although much smaller in effect is the finite amount of charge necessary to trigger the discriminator. In general, after reaching the discriminator threshold, a certain amount of charge must be integrated on a capacitor before a logic signal is emitted.

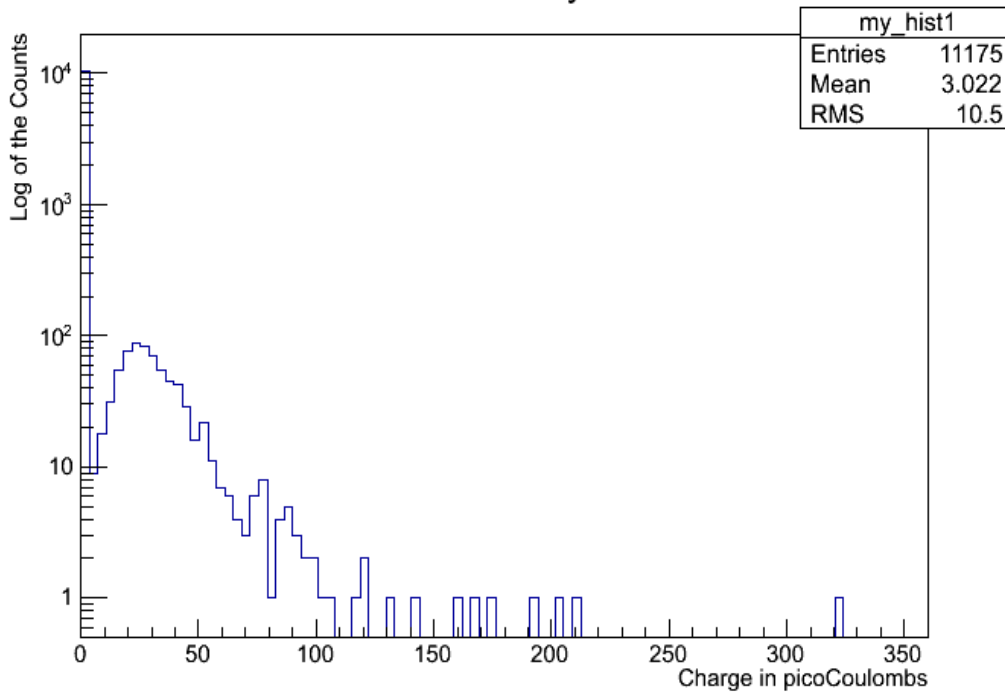
Timing fluctuations are also caused by noise and statistical fluctuations in the original detector signal. Because of these random fluctuations, two identical signals will not always trigger at the same point, giving instead a time variation dependent on the amplitude of fluctuations. This effect is usually referred to as *time jitter*.

### ANALOG TO DIGITAL CONVERTER

The input signal is first used to charge a capacitor. The capacitor is then “run down” i.e. discharged at a constant rate. At the start of the discharge, a scaler counting the pulses forms a constant frequency clock or oscillator is gated on. When the capacitor has completely discharged, the scaler is gated off. The content of the scaler is then a number proportional to the charge on the capacitor.

## Charge Histograms

Data on 16 May 2012



Data on 17 May 2012

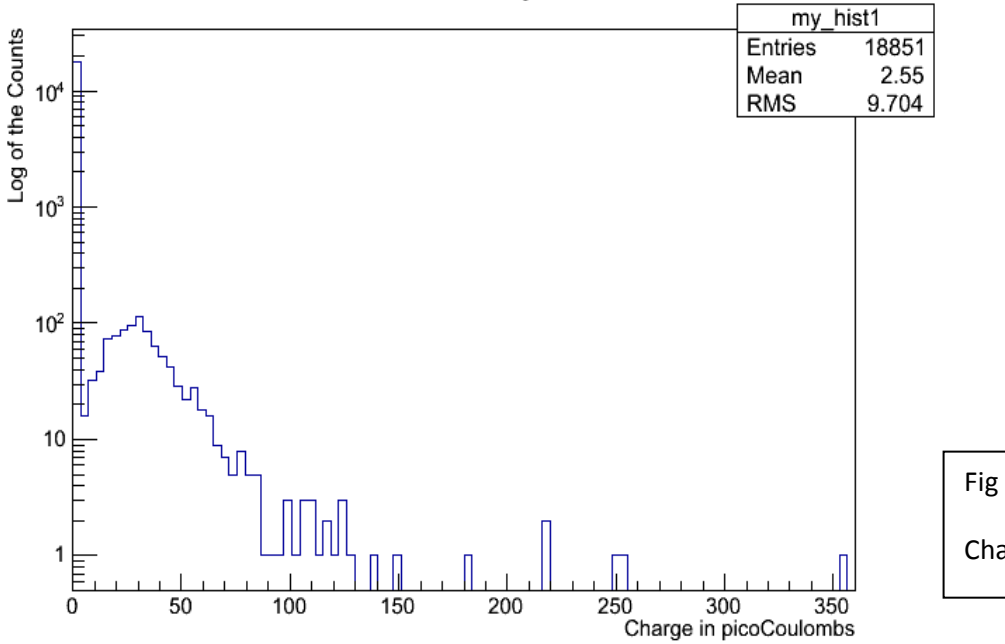


Fig 7 and Fig 8:  
Charge histograms

Fig 7 and 8 represent the charge deposited in the scintillator by the muons. The peak at zero is the pedestal, i.e when no particle passes through the detector. The scintillator used had 4 fibres in a sigma shape. Hence a storage oscilloscope was needed as the signal was very weak. The charge was calculated by finding out the area under the voltage curve and dividing it by the resistance value (50 ohms).

## Mounting a scintillation detector

The scintillator used was 31 cm wide with 30 grooves each of thickness 5mm. Each of these grooves contains five optical fibres.

### Step 1:

The scintillator was cleaned properly. Alcohol (Propan-2-ol) was used for this purpose.

### Step 2:

The optical fibres were cut to the desired length. Five of such fibres were taken at a time and fitted in each of the grooves of the scintillator. They were fixed to the scintillator by means of Aluminium tape and glue. The glue used was E-30 CL Hysol. This glue was allowed to dry for almost a day.

### Step 3:

The parts of the fibres hanging out of the scintillator were inserted into an acrylic cookie and then glued to it. It was then covered with black tape to avoid any unwanted material getting stuck to it. This was also allowed to dry for a day.

### Step 4:

The extra length of the fibres, the parts that were hanging out were cut and the edges of the scintillator were polished. The surface of the cookie was also polished.

### Step 5:

An aluminium strip was fixed at one edge of the scintillator (the one away from the long end of the fibres). This serves as a good reflector. The scintillator was then covered in white "TYVEC" paper. Since the light is emitted isotropically by the scintillator, it must be reflected back to avoid losses. The Tyvec paper aids in this. The Tyvec paper was held in place by means of Aluminium tape and black tape.

### Step 6:

Next, it was covered with several layers of black Tedlar paper. This was also fixed by means of black tape.

### Step 7:

A Photo-multiplier tube was attached to the acrylic cookie. It was fixed by means of black tape. The entire scintillator paddle was covered extensively with black tape to avoid any external light from entering into it.

### Step 8:

The scintillator was fixed onto a wooden board to keep it firm and stable. By now, the scintillator was completely ready for data collection.

Since this scintillator has 150 fibres, it was directly connected to the ADC and the storage oscilloscope was not used. However due to the 20 metre cable used to adjust the timing delay the signal was highly attenuated.

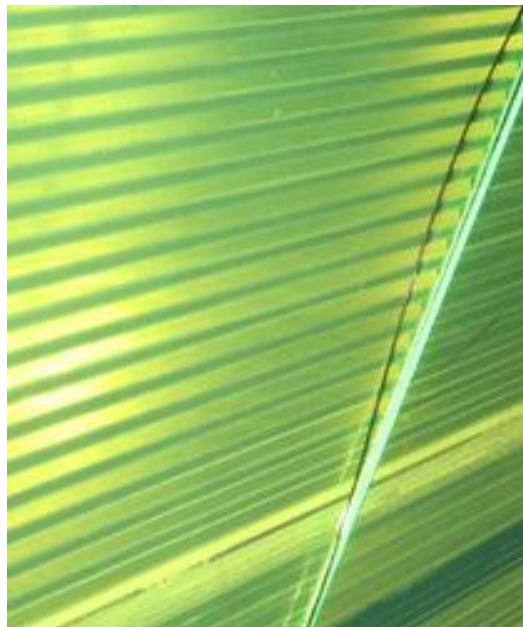


Fig 9: The scintillator as it looks with the fibres fitted in the grooves. Each groove is 5mm wide and contains 5 fibres.



Fig 10: The scintillator paddle after packaging. A PMT is attached to the acrylic cookie. The scintillator and the PMT are covered extensively with black tape to avoid any leakage of light.

Some pictures of the scintillation detector that we made

# Characterisation of the RPCs

## V-I Characteristics

V-I characteristics for channel a

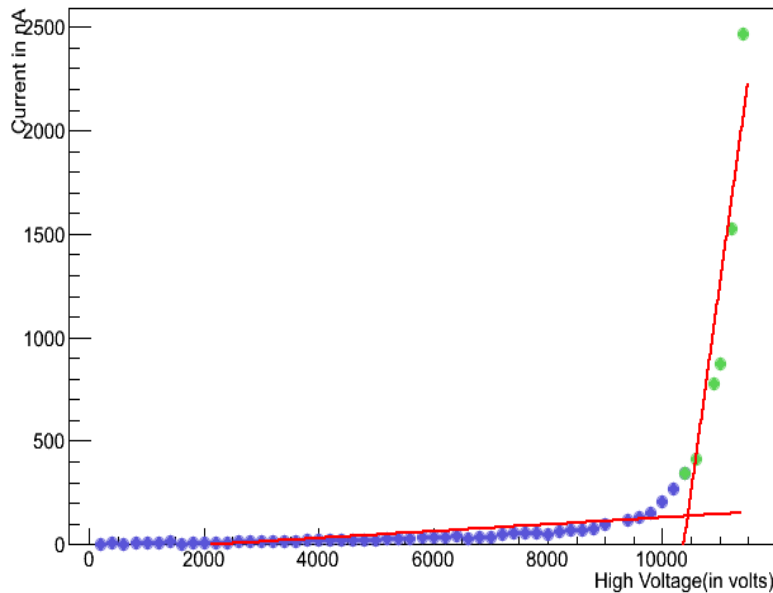


Fig 11: V-I Characteristics for Channel A

V-I characteristics for channel b

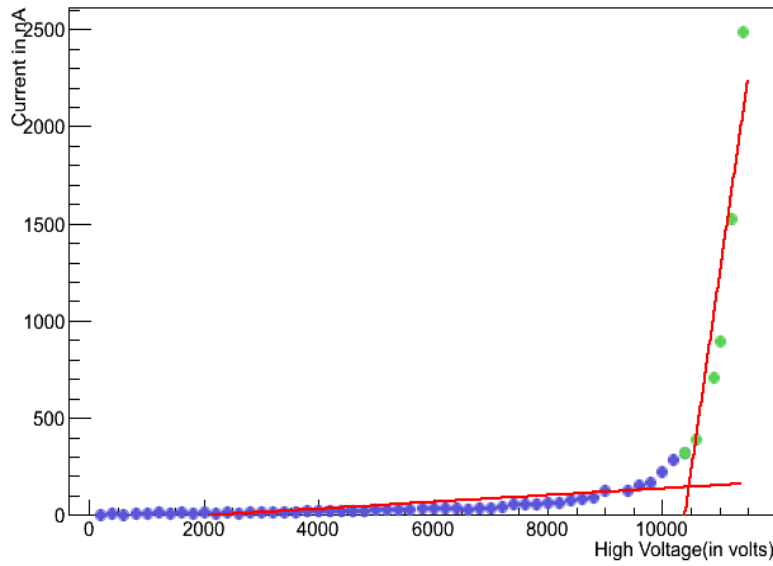


Fig 12: V-I Characteristics for Channel B

Fig 10 and 11 represent the variation in the current as the applied voltage is changed. Equal and opposite voltages were applied at the two channels- A and B and the corresponding current values were observed. The current values were almost the same.

Channel A: Glass Resistance:  $0.502 \text{ G}\Omega$

Gap resistance:  $60.22 \text{ G}\Omega$

Channel B: Glass Resistance:  $0.489 \text{ G}\Omega$

Gap resistance:  $57.3 \text{ G}\Omega$

## Efficiency and Noise Rate of the RPCs

The efficiency of RPC is calculated with respect to the scintillator paddles as reference. Two such paddles were used in order to provide a two-fold coincidence (2F). A trigger would be produced when a muon would pass through both the paddles. The signal from each scintillator was sent to a discriminator (with a threshold of -30 mV) to convert the analog pulse into a NIM pulse. The outputs from one of the discriminators with delayed by 150 ns to avoid for jitters. The two outputs were then passed through an AND gate to get a trigger pulse (2F).

For the RPC (AL03), strip 19, 20 and 21 were considered. S20 was the main strip, 19 and 21 being the right and the left respectively. The outputs of the RPC strips were passed through pre-amplifiers and then through discriminators (threshold of -22mV) to get a NIM pulse. These pulses were directly passed to scalars to count the pulses and hence measure the noise rate. The NIM pulses from the RPC strips along with the trigger pulse from the scintillator were given to an AND gate to get the three-fold (3F) coincidence.

The efficiency was calculated by:

$$\text{Efficiency} = 3F/2F * 100$$

For voltages from 9.1kV to 10.1KV the efficiency and noise rate were calculated for runs of two and a half hours each.

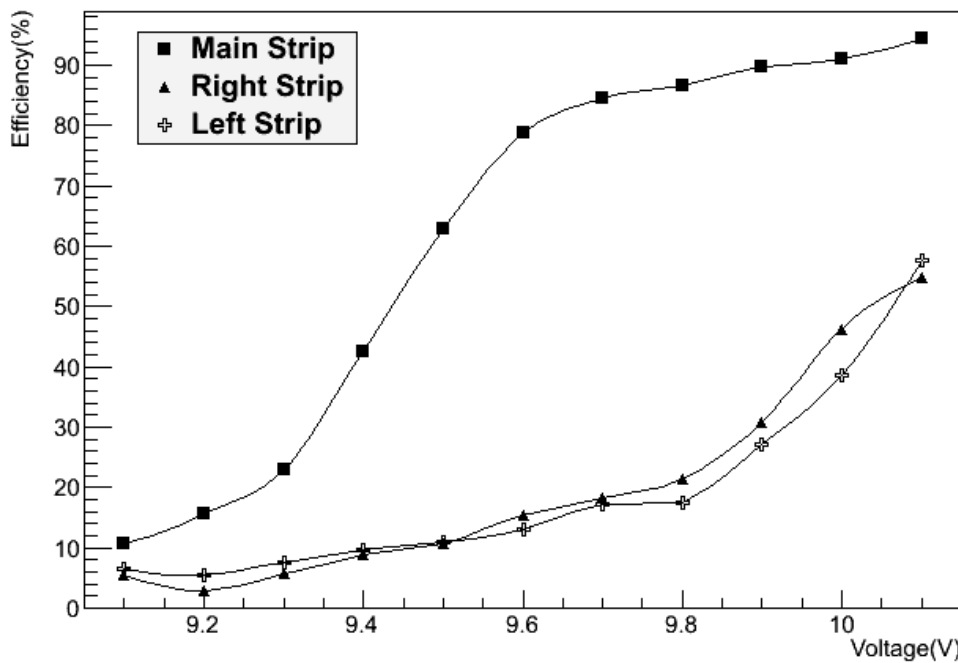


Fig 13: Graph showing the efficiency of the RPC -strip 20 (main), strip 19 (right), strip 21(left) as a function of the high voltage applied. With increase in the high voltage applied the efficiency for the RPC increases. However, there is a plateau region beyond 9.8kV which is optimum for the usage of the RPC, where the efficiency remains constant with increase in voltage.

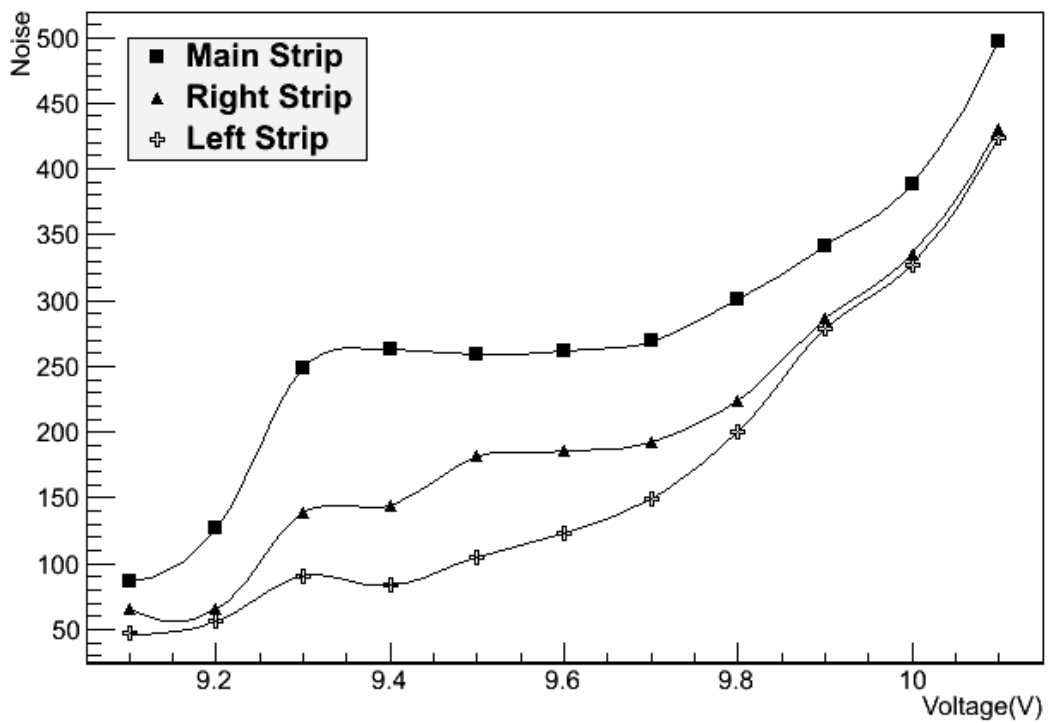


Fig 14: The above graph shows the variation of noise in the RPC as the applied high voltage to the RPC is varied. As the high voltage increases, the noise rate also increases. The noise rate of the main strip is clearly more than the left and the right one.

#### NOTE:

The data for efficiency and noise rate of the RPC was taken twice. In the first attempt, the noise rate was exceptionally high, so the desired results were not obtained. The high noise rate was due to presence of stray cables since two of the RPCs in the setup had been disconnected.

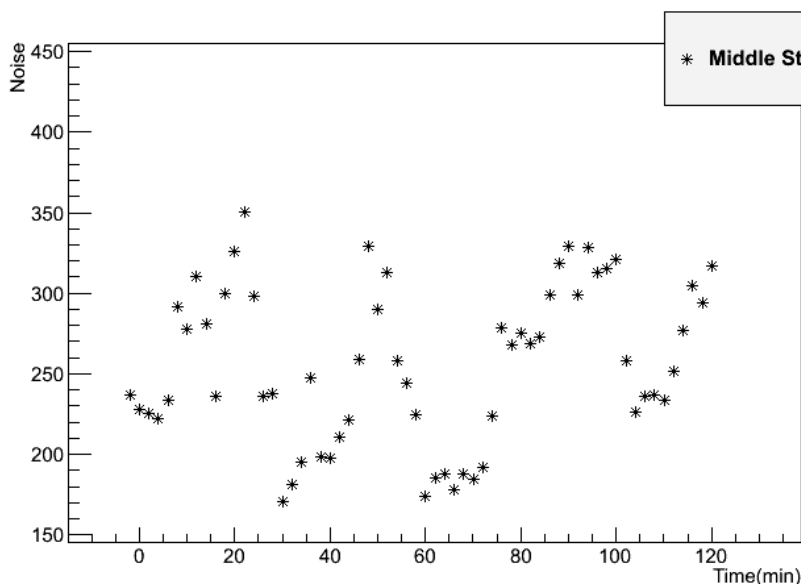


Fig 15: A typical noise vs time plot. This plot shows how the noise rate varies as a function of time. Clearly the noise rate is random.

## Some examples of the hit data

Fig 16: This figure shows the positions of hits in each layer. The X-axis shows the positions of the layers and the Y-axis shows the positions of the strips (in cm) that are hit. These graphs are for the X-side pick-up panel.

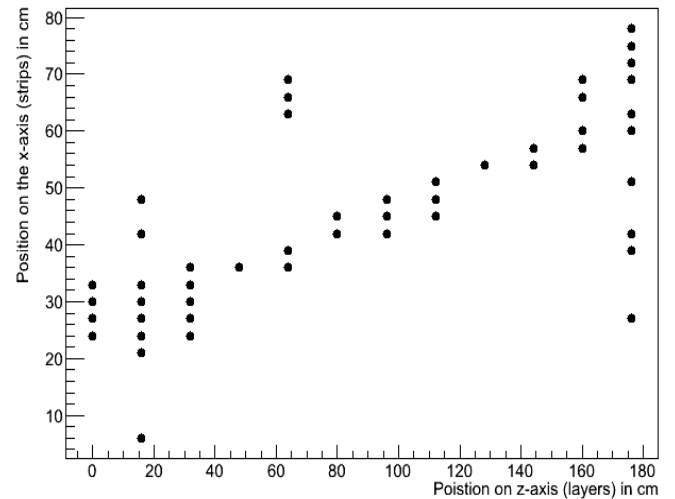
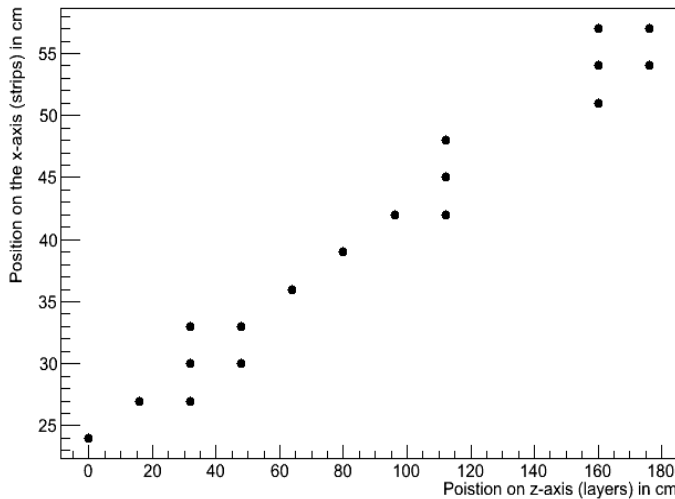
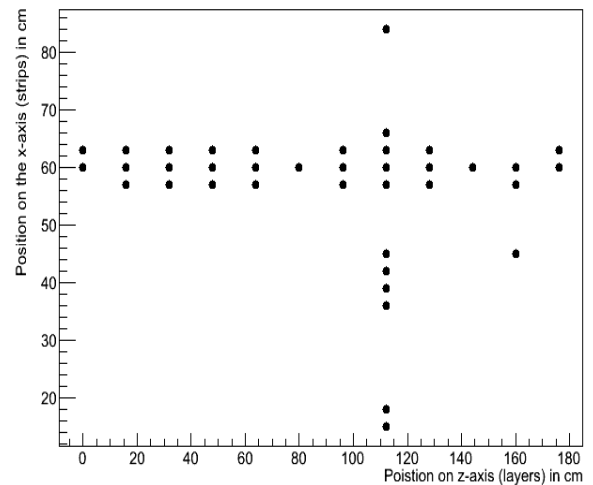
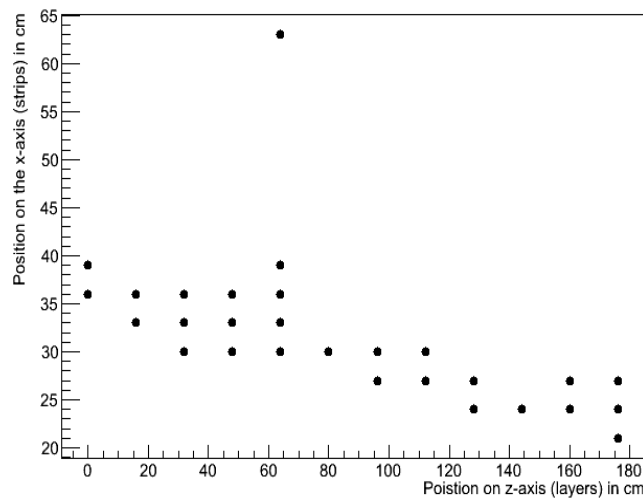
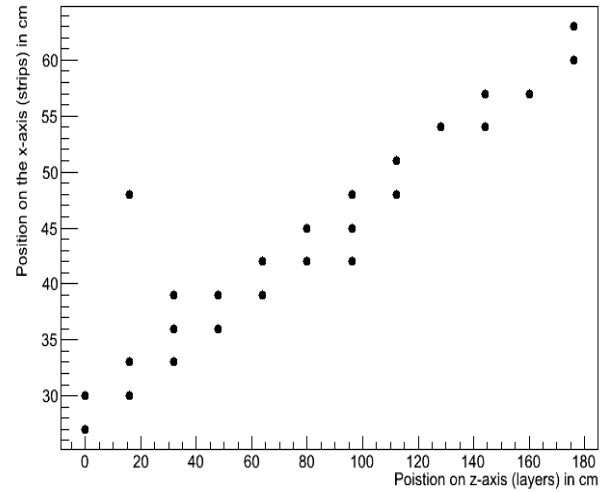
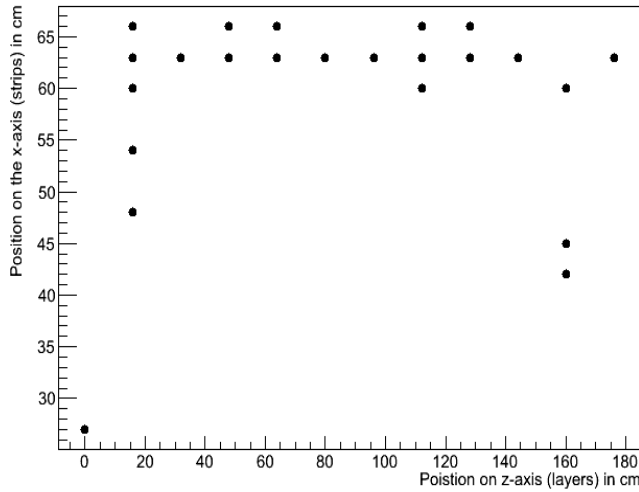
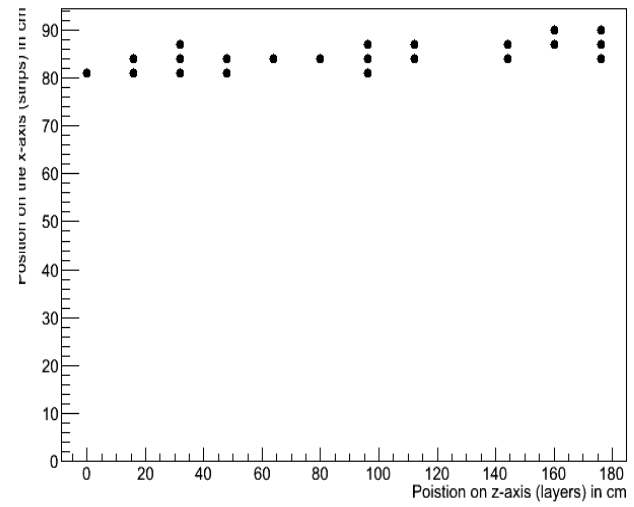
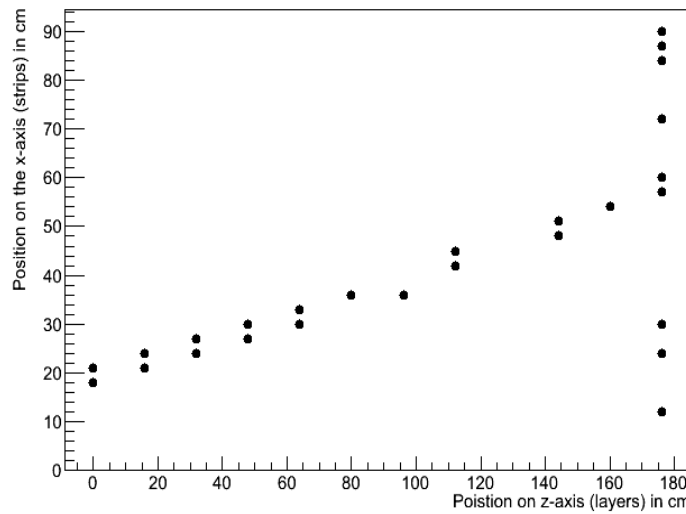
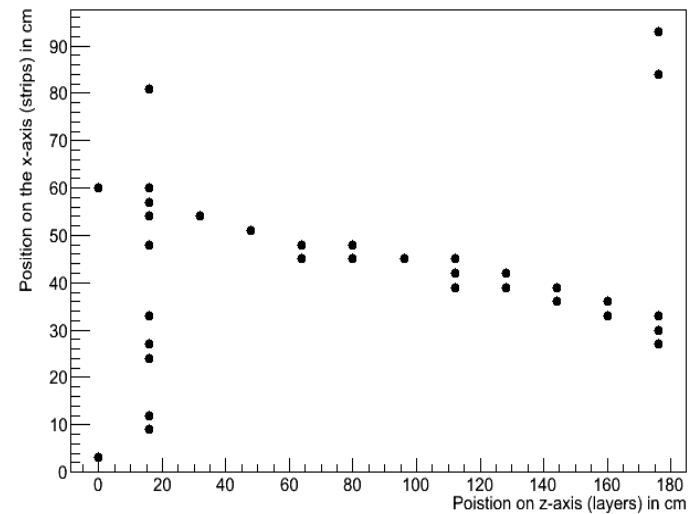
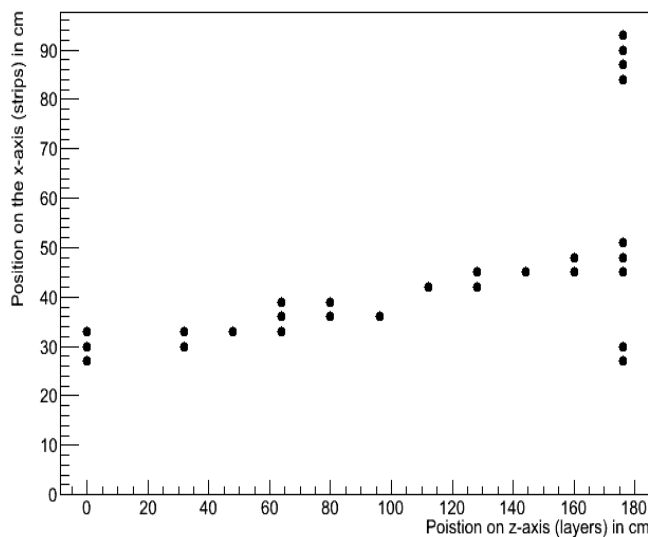
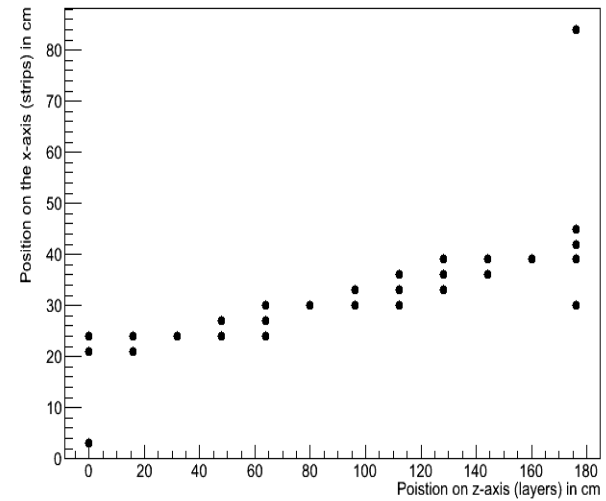
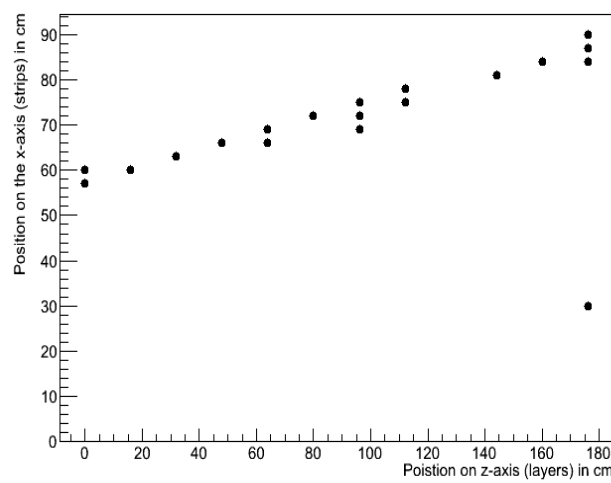


Fig 17: This figure shows the positions of hits in each layer. The X-axis shows the positions of the layers and the Y-axis shows the positions of the strips (in cm) that are hit. These graphs are for the Y-side pick-up panel.



# Reconstruction of muon tracks

## Tracking Algorithm

- Consider only those layers in each event which have a maximum of three hits, to reduce the number of combinations possible. These are the non-noisy layers.
- Consider only those events which have at least four such layers.
- Hence, for the rest of the analysis, all the events considered have at least four layers with at most three hits each.
- Consider all possible hits between the first and the last non-noisy layers . Since the layers can have more than one hit, several combinations are possible.
- Find the slopes and intercepts for all possible combinations of hits in these layers. This gives several possible values of slopes and intercepts.
- Using these different values of slopes and intercepts, get different track candidates.
- Use the track candidates to get the estimated positions for hits in each layer.
- Now, using the values of the observed positions and the estimated positions calculate the residues and hence the chisquare values for each of the estimated lines.
- Choose the line which has the minimum chisquare value.
- Now, there is ONE line which is the best fit line.
- Next, find the hit position that is closest to this estimated line.
- Using the closest hit position and the estimated positions, get the residuals and the chisquare value.
- If the chisquare value is less than 4.5, keep this line. Else, try the same procedure with a new combination of layers.
- Again check the final chisquare value (from the positions of closest hit), if it is greater than the previous one, retain the previous one. If it is less than the previous one, update the value of chisquare. If chisquare is still quite high i.e. greater than 6, try the same procedure with another combination of layers.
- Finally retain the chisquare value that it is the least out of the three that were calculated.
- Use the final residuals and chisquare value to plot histograms.
- Finally, plot the track which corresponds to the minimum value of chisquare out of the three calculated ones.
- Plot the hits and overlay the fitted line for the track.

## Plots for no of hits in each layer

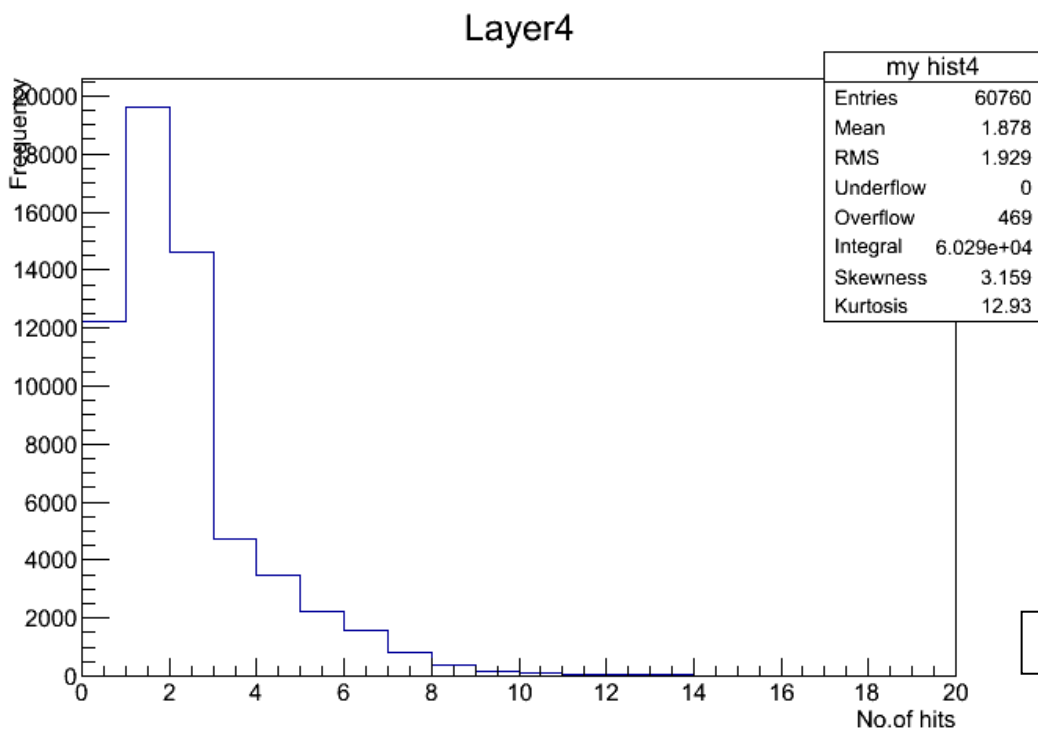
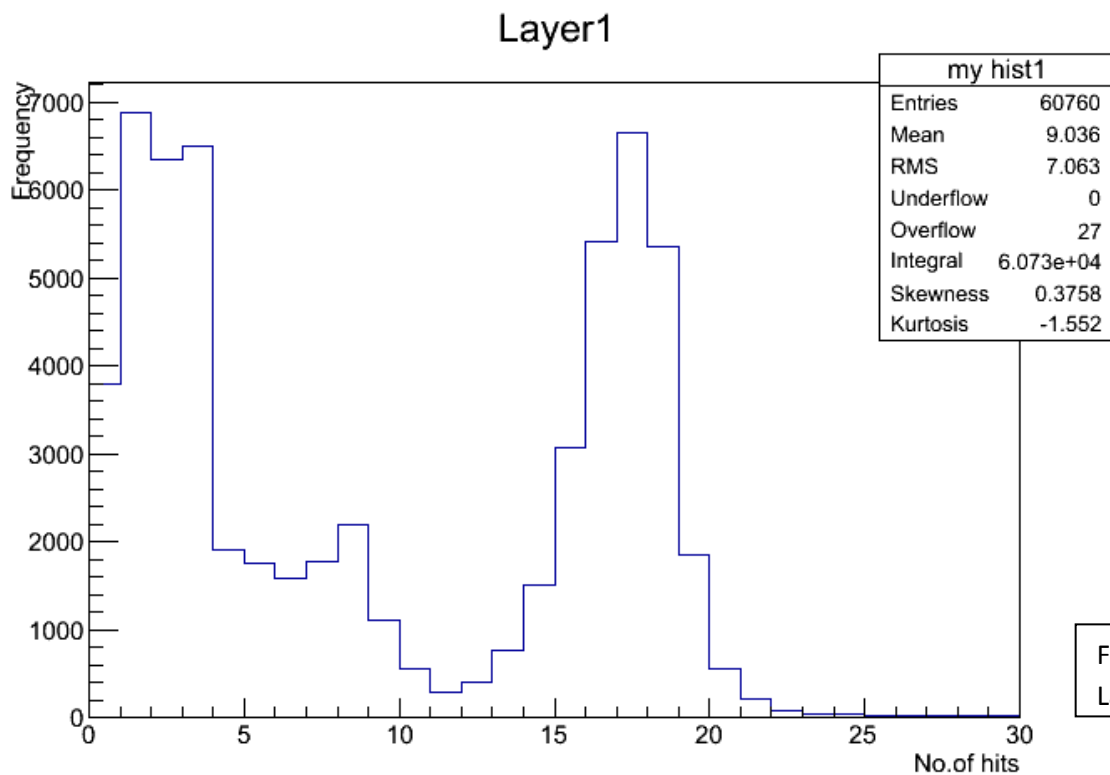


Fig 17: Histograms for hits in layer 1. It shows a large no of hits.

Fig 18: It shows the histogram for the hits in layer 4.

In many events, these are two of the noisy layers.

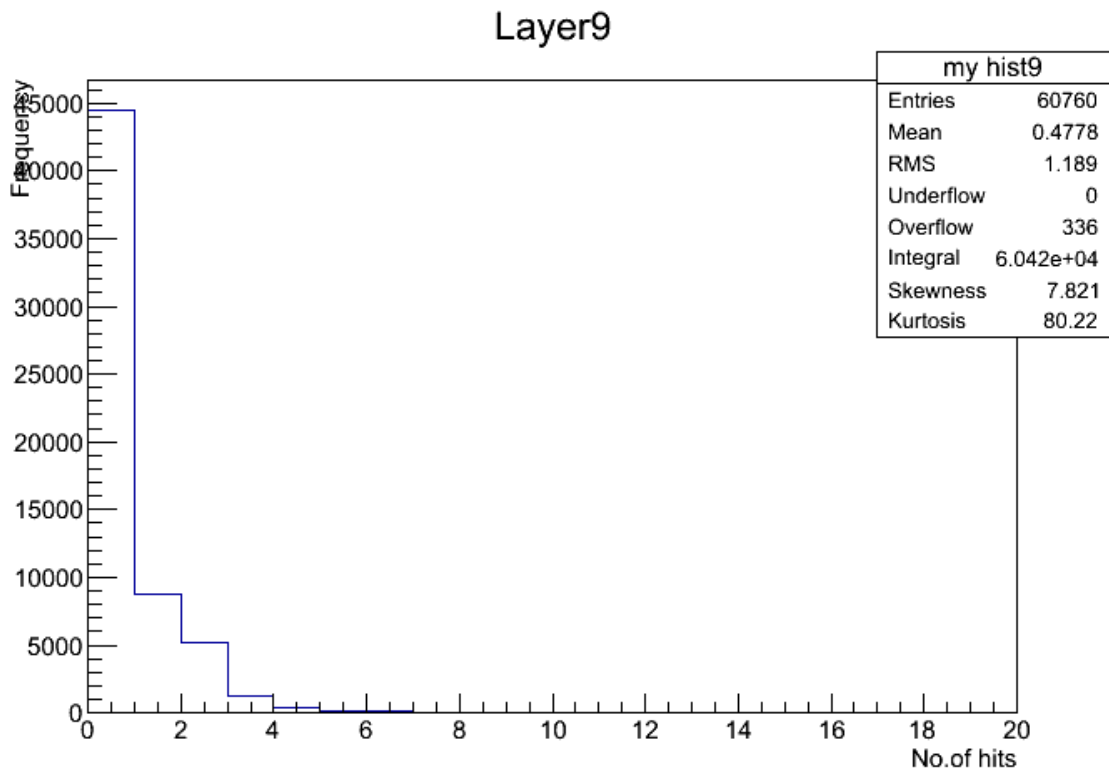
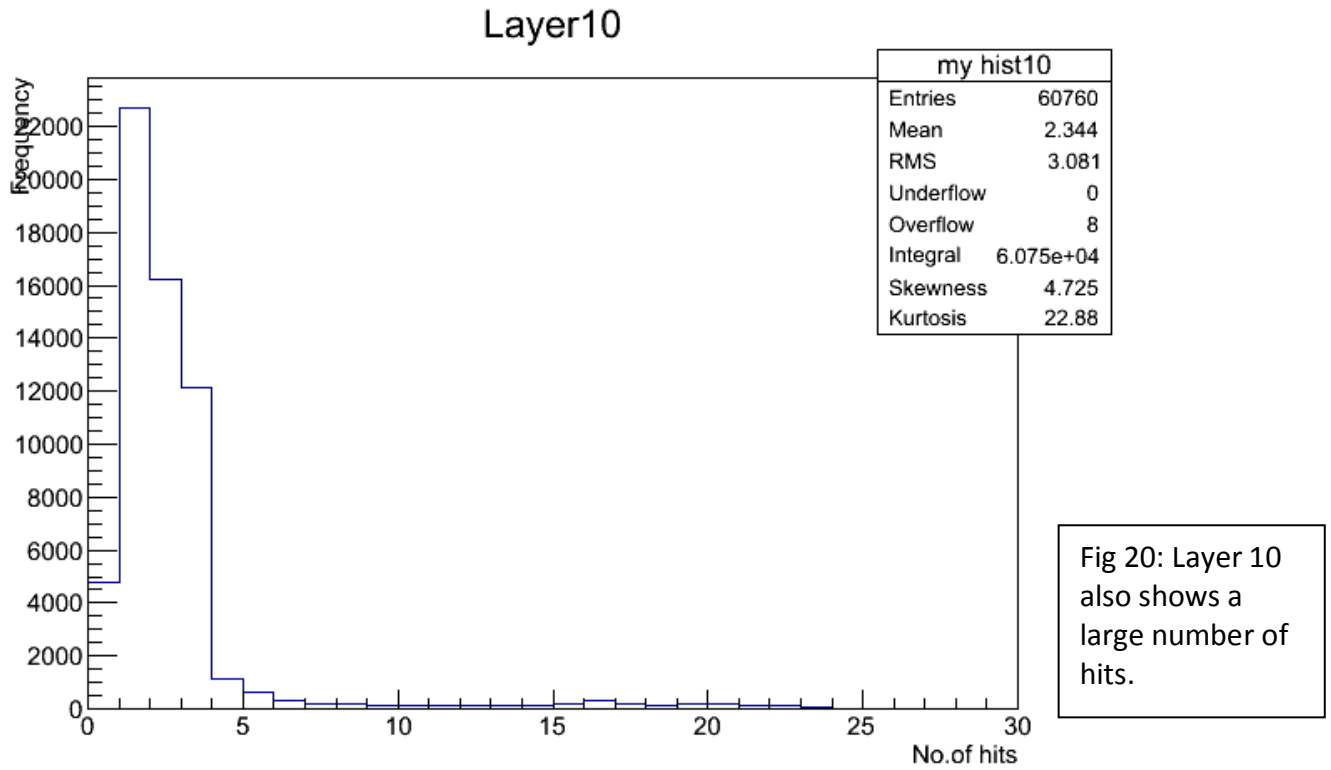


Fig 21: Layer 9 is a typical layer. All the layers that are not noisy show a similar pattern for the number of hits. As the layers 1, 4 and 10 show a much larger number of hits than the others, these are hence the noisy layers. Next we try to eliminate the layers with more than three hits (the noisy layers). This is exhibited in the next two histograms.

## Plot for total number of layers that are hit in each event

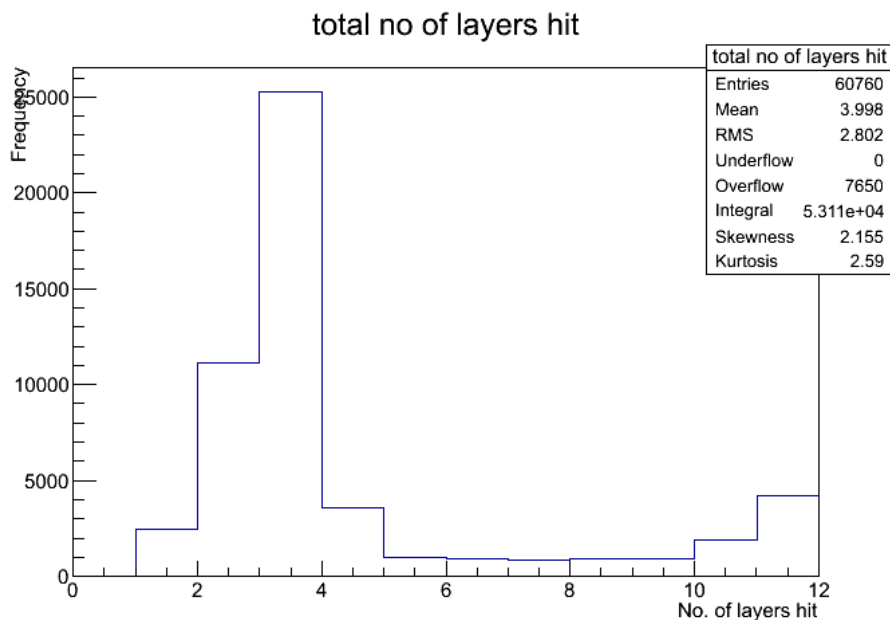


Fig 22: This histogram shows the no of layers that are hit in each event. Very few events have all the layers hit; these are the ones that correspond to the muons. A lot of them have few layers being hit. This is either due to electronic noise or something to do with the pre-amplifiers.

## Plot for the no of layers being hit at most thrice

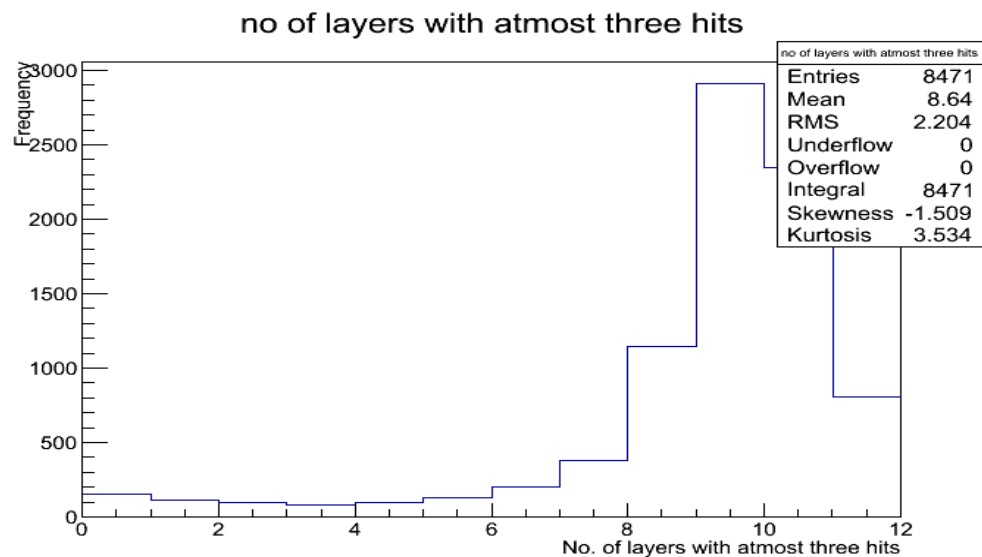


Fig 23: This shows the number of layers in each event that have a maximum of three hits. Since, I want to reject the noisy layers; I have looked at a histogram for the layers that have a maximum of three hits. Only such events which have atleast 4 such layers would be considered for reconstruction of the muon tracks.

## Plot for the chi square values

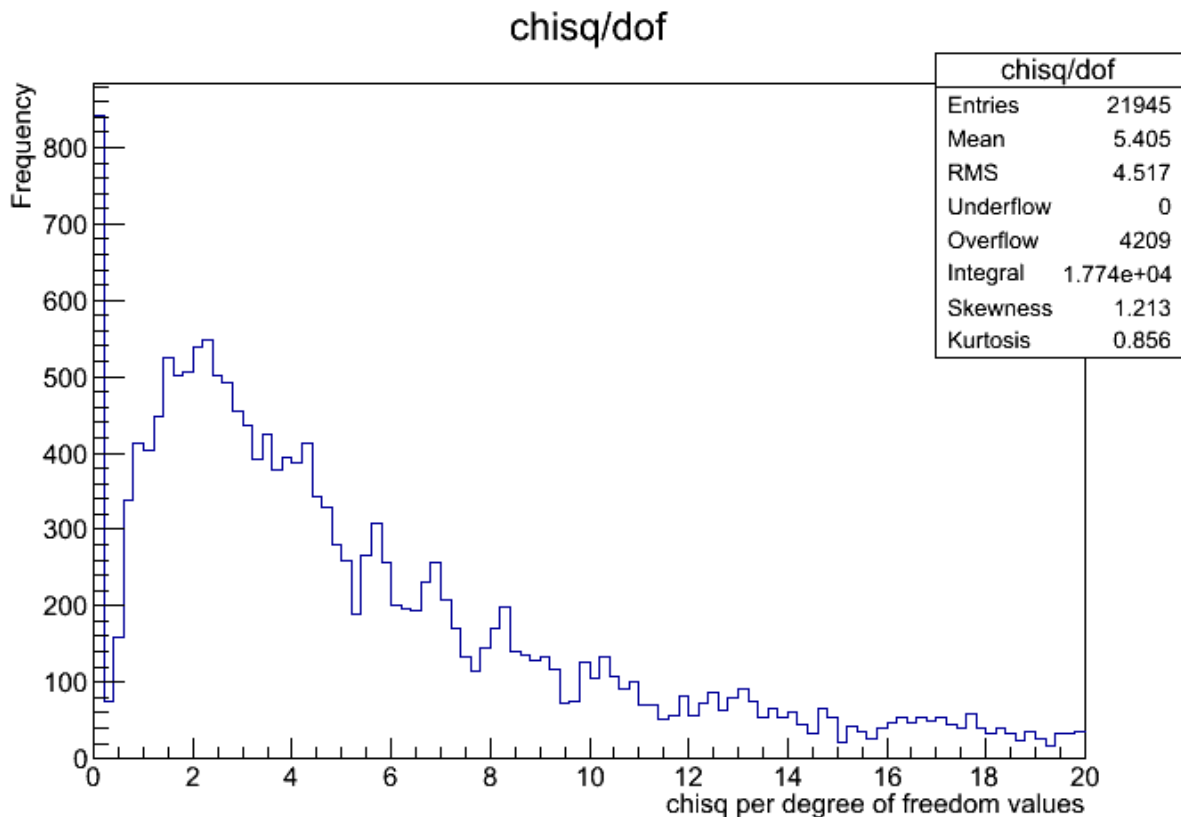


Fig 24: The X-axis represents the value of the chi square per degree of freedom, and the Y-axis represents the frequency of the chisquare/dof values. Most of the tracks have good chi square values (i.e less than 4).

The chi square value is defined as:

$$\chi^2 = \sum (\text{observed} - \text{expected})^2 / \sigma^2$$

where the quantity in the brackets is called the residue and  $\sigma$  is the error in the measurement.

Chi square per degree of freedom is calculated by  $\chi^2/12$ .

The number 12 is used because there are as many layers in the detector.

A best fit line (the one with the least chisquare per dof value) was estimated from the combinations of hits arising from the first and the last non-noisy layer of the RPCs.

The residues (difference between the observed and estimated points) were calculated for the closest hit in the good layers (with a maximum of three hits).

The chi square values per degree of freedom were hence obtained.

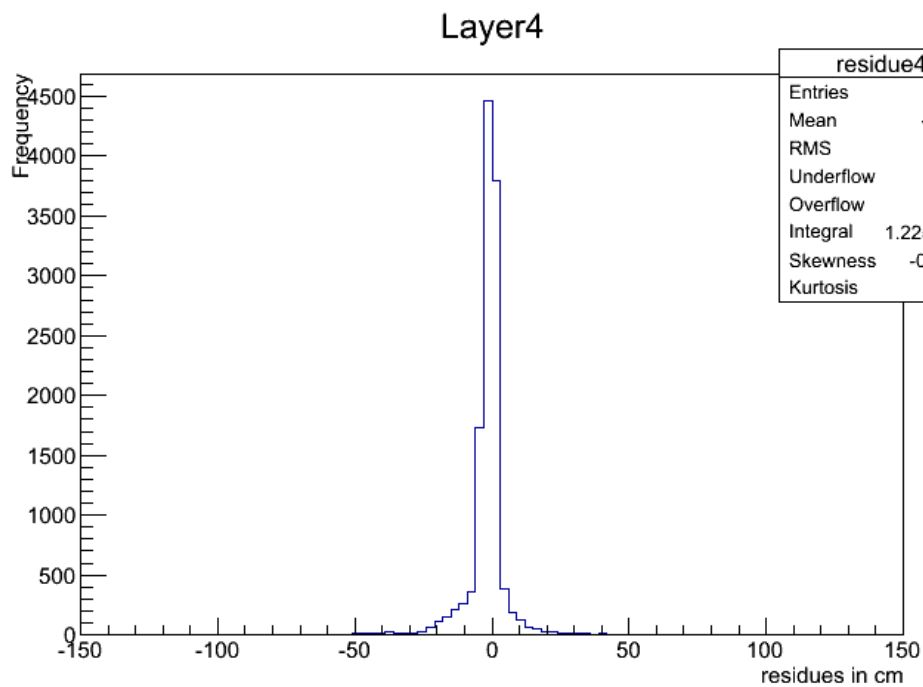
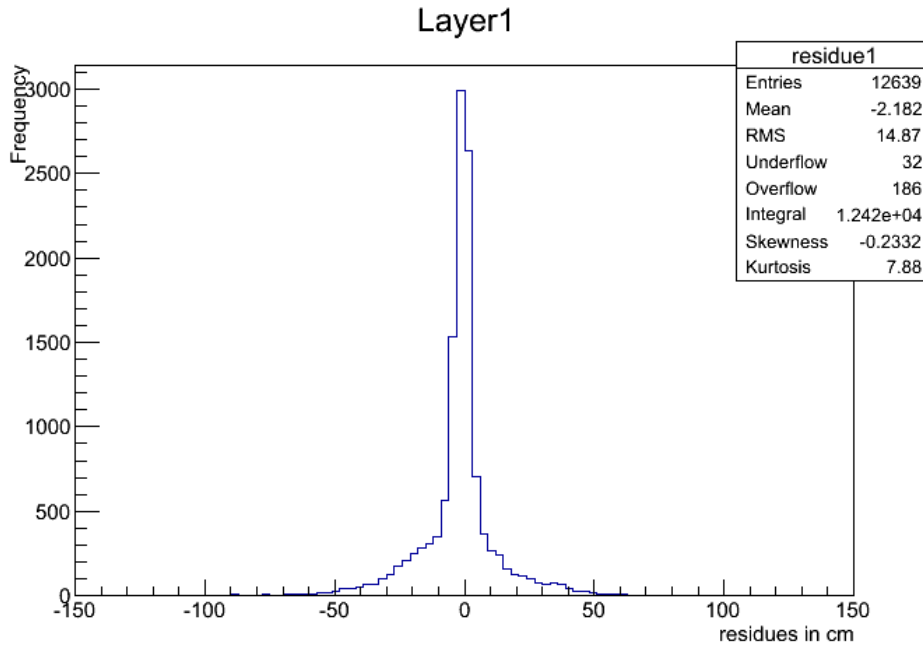
If the chisquare per dof value was greater than 4.5, a different combination of layers was used. If the new chisquare per dof value was lesser than the previous one, it was retained, else it was rejected. Again, if the new chisquare per dof value was greater than 6, a different combination was tried. Finally the line with the least chisquare per dof value was retained.

## Residual plots

The residual plots were made for the hit that was observed to be the closest to the best fit line.

$$\text{Residue} = (\text{closest hit position} - \text{estimated position})$$

The subsequent plots show the residuals for individual layers.



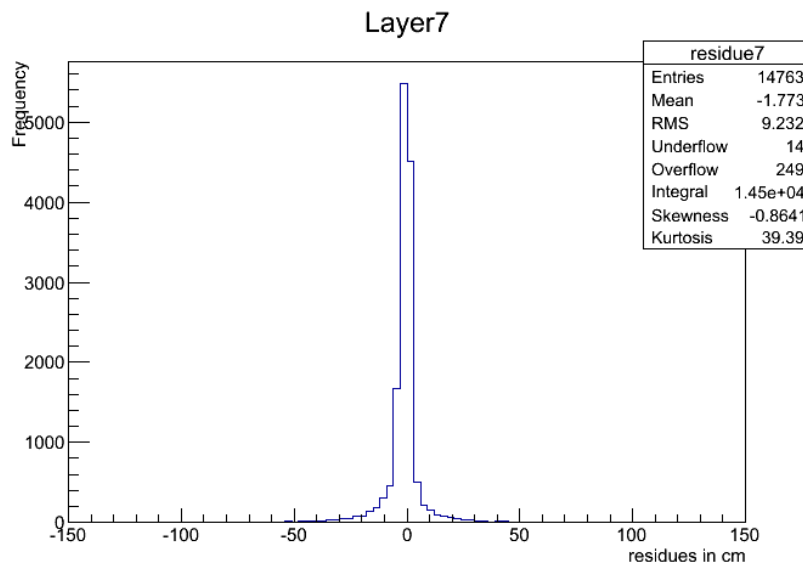


Fig 27: Residual plot for layer 7

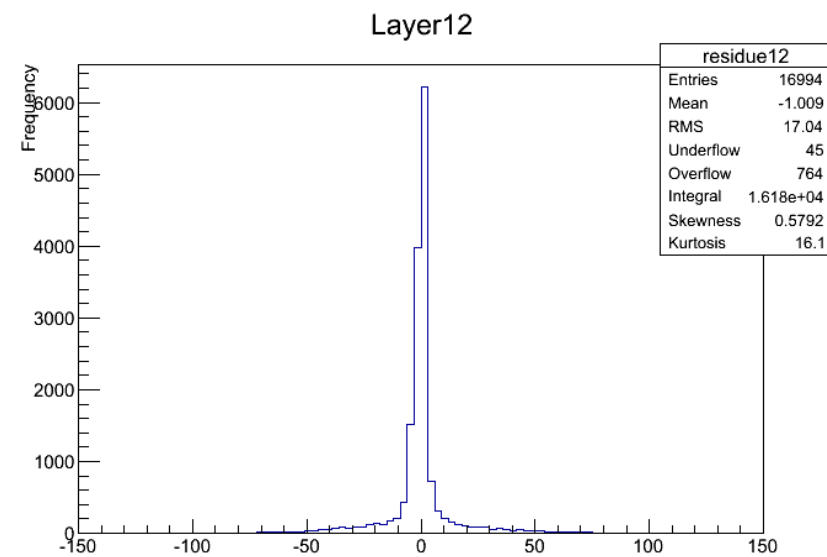


Fig 28: Residual plot for layer 12

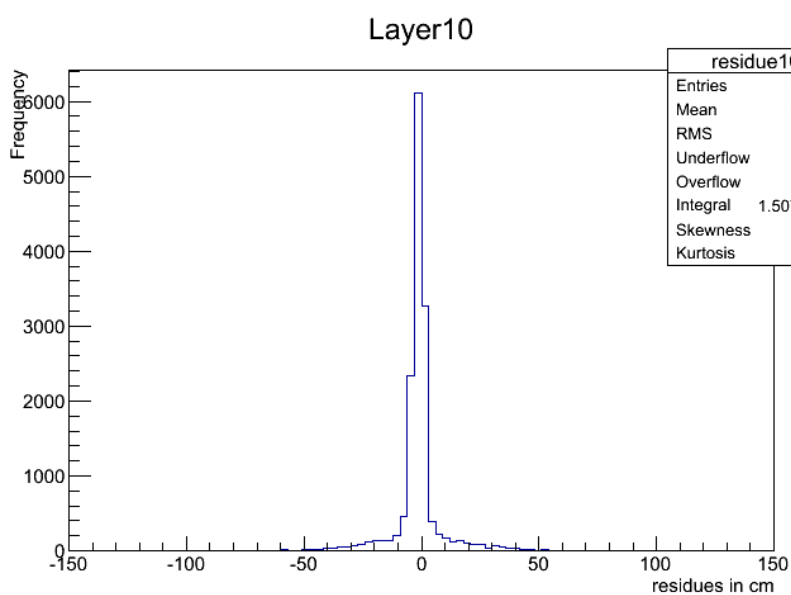


Fig 29: Residual plot for layer 10

# Tracks along with the hit data

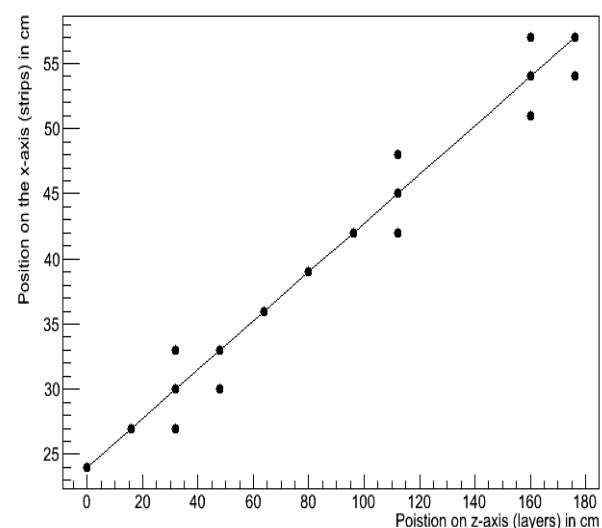
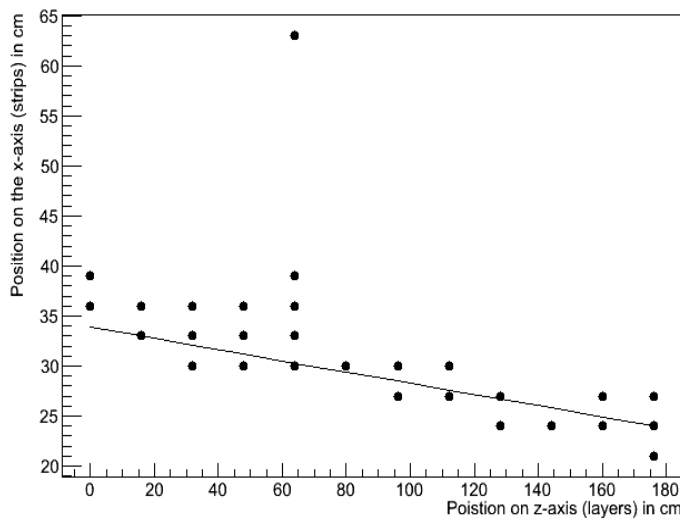
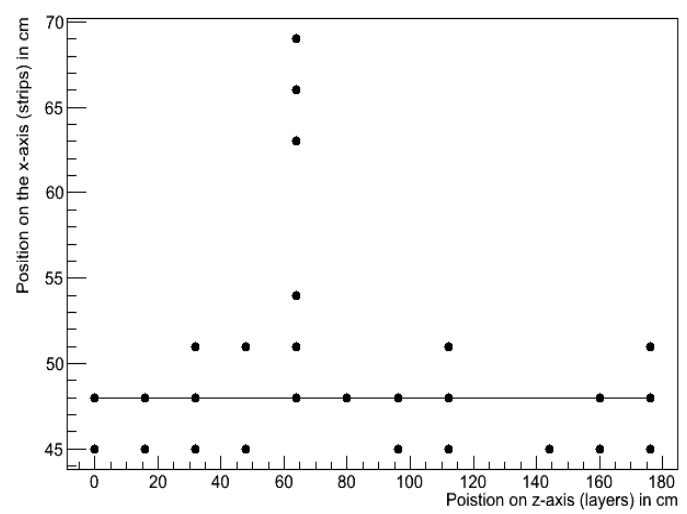
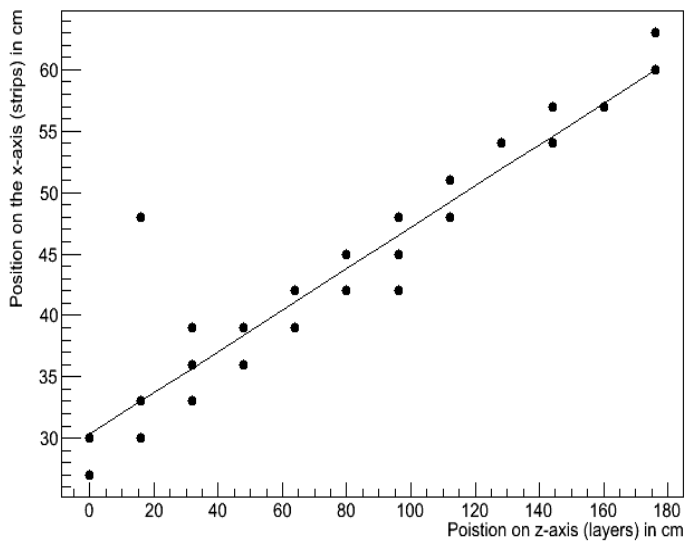
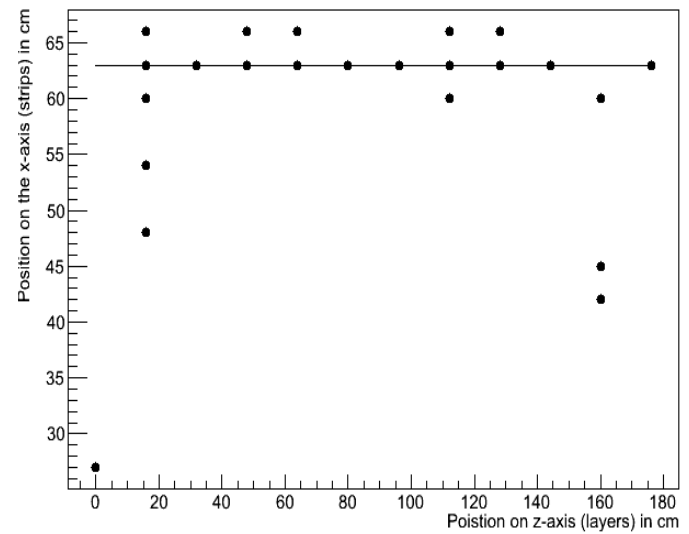
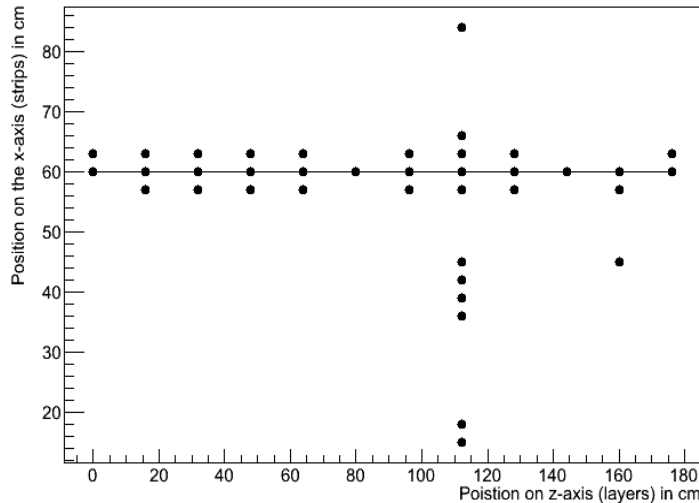


Fig 30: It shows the hit data along with the tracks estimated.

## Some of the events with bad tracks

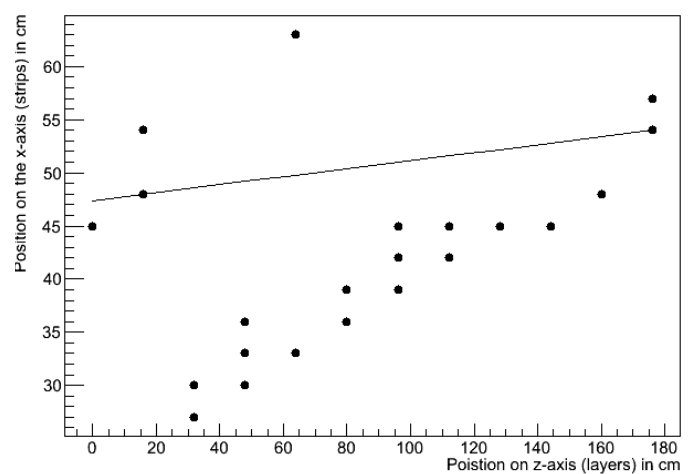
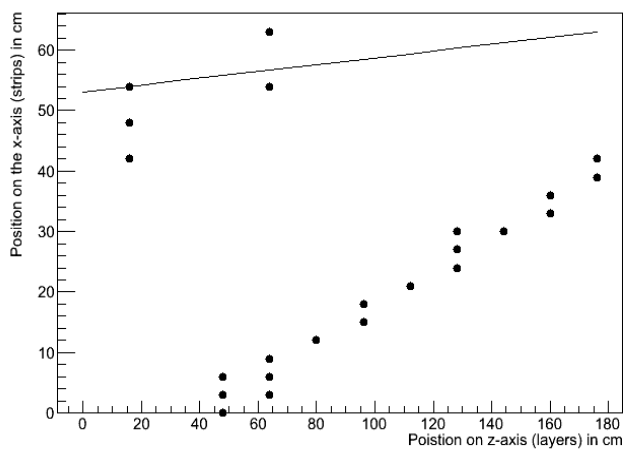
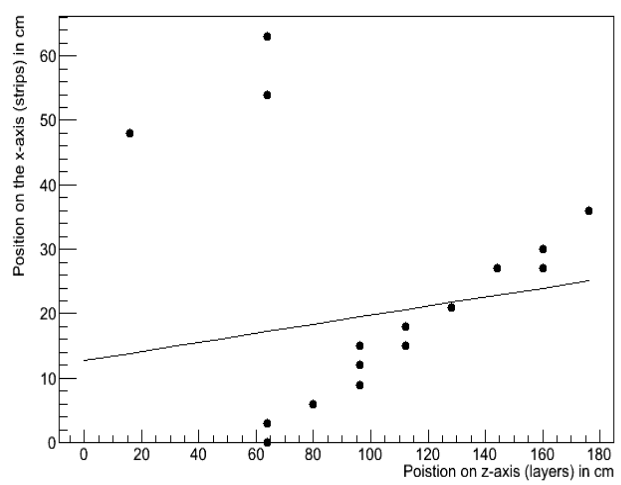
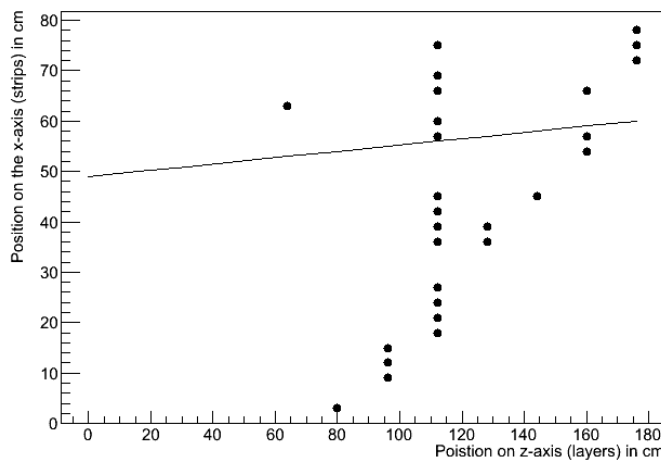
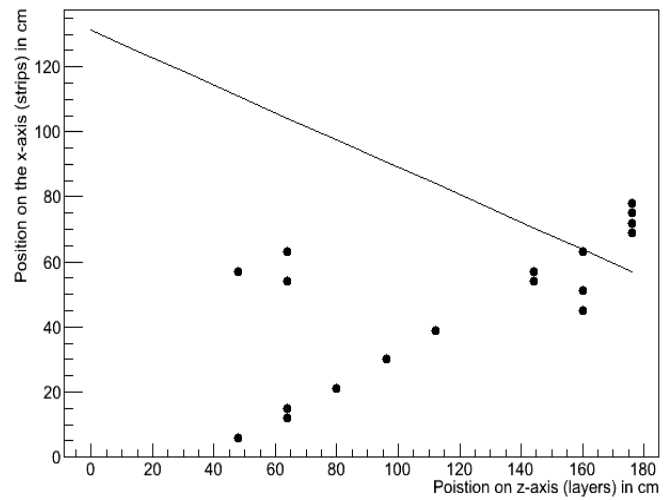
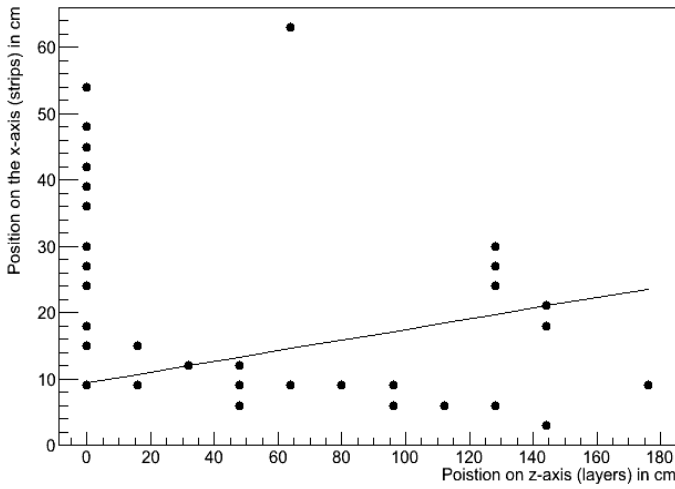


Fig 31: This figure shows some of the bad tracks. Most of the events have hits only in the later layers and the algorithm uses the initial layers as well for fitting, that is mainly why these tracks have gone bad. They could also probably be fitted by choosing a different combination of layers.

## Results and Discussions

Hence, during the course of this project I worked with the scintillation detector and the gas based RPCs. I was also involved in the packaging of a scintillation detector.

I studied the distribution of charge in the scintillator as particles pass through it.

Next, I worked with the RPCs. I studied its characteristics- variation of current, efficiency and noise rate as a function of the applied voltage.

The major part of my project was analysis of the data collected for the muon events. I constructed an algorithm to reconstruct the track of the muons passing through the RPC and implemented it. Out of 21945 events possible, only 4209 events give chisquare values higher than 20. Most of the events give a chisquare value less than 4 which implies that the fitting algorithm is fairly efficient.

## Acknowledgements

I am grateful to my project advisor, Professor Sudeshna Banerjee, for giving me a chance to work under her guidance. I am greatly indebted to her for guiding me at each step. She has always been a source of inspiration that made me work hard. It is only because of her enthusiasm, inspiration, sound advice and great efforts to explain things clearly and simply, that this project has been possible.

I am also thankful to Mr. L V Reddy, R. R. Shinde, Sumanta Pal, Sudeshna Dasgupta and all the members of the lab.

I am also thankful to my friends, Divya, Harsha and Abhilasha, for making my stay at TIFR a pleasant one.

## References:

- ❖ Design and Characterisation Studies of Resistive Plate Chamber by Satyanarayan Bheesette
- ❖ Techniques for nuclear physics and particle physics experiments by W.R. Leo
- ❖ [www.google.com](http://www.google.com)
- ❖ [www.tifr.res.in/~bsn](http://www.tifr.res.in/~bsn)